Journal of Non-Crystalline Solids 357 (2011) 3480–3485

Contents lists available at ScienceDirect

Journal of Non-Crystalline Solids

journal homepage: www.elsevier.com/ locate/ jnoncrysol

Synthesis and characterization of amorphous aluminosilicates prepared by sol–gel to encapsulate organic dyes

O. Martínez-Zapata [a], J. Méndez-Vivar [a,*], P. Bosch [b], V.H. Lara [a]

[a] Universidad Autónoma Metropolitana-Iztapalapa, Depto. de Química A. P. 55-534 México, D. F. 09340, México
[b] Instituto de Investigaciones en Materiales, Universidad Nacional Autónoma de México Circuito Exterior s/n, Ciudad Universitaria, D. F. 04510 México

ARTICLE INFO

Article history:
Received 18 February 2011
Received in revised form 14 June 2011
Available online 11 July 2011

JEL classification:
C90 - General
C91 - Laboratory, Individual Behavior
C99 - Other

Keywords:
Amorphous aluminosilicates;
Alizarine;
Carminic acid;
Encapsulation;
Sol–gel

ABSTRACT

We synthesized via the sol–gel process three amorphous aluminosilicates having the stoichiometry of zeolite types A, X, and Y, respectively. The aluminosilicate, so-called SX, having the chemical composition of faujasite X, proved to be amorphous in the range 298 K up to 1273 K. At the higher temperature the sample begins to crystallize as nepheline. The anionic organic dye 1,2-dihydroxyanthraquinone (Alizarine, AL) was successfully encapsulated in the aluminosilicate matrix SX. Still, 7-α-D-glucopyranosil-9,10-dihydro-3,5,6,8-tetrahydroxy-7-methyl-9, 10 dioxanthracene carboxylic acid (carminic acid, CA) could only be deposited on the matrix surface. The adsorbents and the dye impregnated matrices were characterized using several techniques: Fourier Transform Infrared (FTIR) and Diffuse Reflectance Spectroscopies used to determine the hydroxylation as well as the adsorbed species, Small Angle X-ray Scattering (SAXS) to know the shape of the heterogeneities and the fractal dimension of each sample, nitrogen physisorption to measure the specific surface area and X-ray Diffraction (XRD) to identify the crystalline compounds present in the samples. Therefore, with these complementary techniques, the structure and the morphology of the samples were obtained.

1. Introduction

The mild conditions of the so-called soft chemistry processes allow the design of organic, inorganic and hybrid materials. The hydrolysis–condensation reactions of metal alkoxides used as precursors in the sol–gel process lead to the synthesis of porous inorganic matrices such as aluminosilicates. The porosity of the final material can be tailored to obtain membranes, molecular sieves, catalysts, sensors, etc. [1–5].

Currently, there is a great interest in the cleaning of streams from industries, such as those involved in the printing and textile processes [6–8]. One strategy is to encapsulate the dye molecules in porous matrices such as aluminosilicates via short distance bonding between the functional groups of the dye molecules and those in the cavities of the aluminosilicate [9,10]. In the zeolitic crystalline materials, zeolite types FAU and LTA are known to be those having the largest pore volumes, a property that can be exploited to encapsulate organic dyes [11].

In previous works, layered double hydroxides have been prepared with an azoic dye (methyl orange) stabilized on the external surface. Methyl orange was incorporated by reconstruction from a mildly calcined precursor [12,13]. Similar inexpensive and simple sol–gel (or pyrolysis, dip coating etc.) technique(s) may be used. The molecules entrapped into sol–gel matrices are isolated in an individual cage. Silica has been used as a host matrix and the surface has been modified with ammines, thiols or methacrylate among other compounds to alter the surface. The present study proposes the incorporation of Al to reach a similar purpose.

The goal of the present work is to synthesize via the sol–gel process amorphous aluminosilicates having identical composition as those of faujasites A, X and Y, in order to be used as matrices to host either 1,2-dihydroxyanthraquinone (alizarine, AL) or 7-α-Dglucopyranosil-9,10-dihydro-3,5,6,8-tetrahydroxy-7-methyl-9,10 dioxanthracene carboxylic acid (carminic acid, CA); being both anionic organic dyes. Alizarine been used as a probe molecule because of the interest it presents either as a product of the anthracene photochemical oxidation or as a dye [14].

In previous manuscripts published from other authors [15–17] and ourselves [18] it has been shown that it is possible to trap cationic species in some aluminosilicates. The adsorption of alizarine has been studied on aluminum gels [14]. In general, the higher the activation temperature of the gel is, the higher is the adsorption capacity. The adsorption could be described equally well by the Freundlich and the Langmuir equations. The apparent enthalpy of the adsorption indicated an activated endothermic chemisorption [14].

Another highly fluorescent anthraquinone dye is carminic acid [19]. The formula of carminic acid has been reviewed [20,21] and it has been found that carminic acid is irreversibly adsorbed on fractal surfaces [22]. Thus, it seems interesting to study other gel formulae that may give rise to solid materials whose advantage is that, as waste,

* Corresponding author. Tel.: +52 55 5804 6543; fax: +52 55 5804 4666.
E-mail address: jmv@xanum.uam.mx (J. Méndez-Vivar).

0022-3093/$ – see front matter © 2011 Elsevier B.V. All rights reserved.
doi:10.1016/j.jnoncrysol.2011.06.020

they can be disposed easily; furthermore the resulting hybrid materials may be used as pigments.

In this sense, aluminosilicate gels have been shown to crystallize in the presence of organic templates and aluminum atoms are known to interact strongly with oxygens or π orbitals of carminic acid [12,18,22]. Aluminosilicate gels could be expected to crystallize as zeolites [18,22]. Negative zeolite frameworks are developed and the resulting structure must provide enough space to locate the compensating organic cations [23]. Zeolites need to crystallize a cation to balance aluminum charge. In this work, we chose a monovalent compensation cation (sodium) in A type zeolite which has the highest number of aluminum atoms per silicon atom and in the X and Y type zeolites a divalent cation was chosen (Mg). In this way, the charge distribution in the gel as in the crystalline material is modulated.

2. Experimental

2.1. Synthesis of aluminosilicate SX

The procedure developed by ourselves describes the preparation to obtain 5 g of an aluminosilicate having the chemical composition of faujasite X, via the sol–gel process: 2.5×10^{-4} mol of tetraethyl orthosilicate (TEOS, 98 wt.%, Aldrich) dissolved in 2-butanol (2-BuOH) was slowly mixed in a round bottom flask with 1.0×10^{-4} mol of magnesium methoxide (MMg, 9.8 wt.%, Aldrich) at room temperature. 9.4×10^{-5} mol of aluminum tri-*sec*-butoxide (T*sec*BuAl, 97 wt.%, Aldrich) was added by dropping. An aqueous NaOH (98.5 wt.%, J. T. Baker) solution containing 1.2×10^{-4} mol of NaOH was also added by dropping. The cloudy sol gradually produced was refluxed at 353 K during seven hours. The resulting suspension was filtered by gravity and washed with 30 mL 2-BuOH. Based on the amounts of reactants employed, the nominal composition of the obtained aluminosilicate SX is $Na_{12}Mg_{23}(Al_{59}Si1_{33}$-$O_{384})\cdot26H2O$. The powder was left to dry at room temperature during 12 h and later on in an oven at 523 K during 24 h in air.

2.2. Synthesis of aluminosilicates SA and SY

A similar procedure was followed to synthesize the aluminosilicate SA ($Na_{12}(Al_{12}Si_{12}O_{48})\cdot27H_2O$) and aluminosilicate SY ($Na_8Mg_{23}(Al_{1.5}Si_{30}O_{63})\cdot480H_2O$. All these syntheses are inspired on the conventional synthesis of zeolites, but introducing the sol–gel methodology.

2.3. In situ trapping of dyes

The incorporation of a 1.0 mol% solution of the dyes 1,2-dihydroxyanthraquinone (alizarine, AL) or 7-α-D-Glucopyranosil-9, 10-dihydro-3,5,6,8-tetrahydroxy-1-methyl-9, 10 dioxo-2-anthroxene carboxylic acid (carminic acid, CA) in 2-BuOH was done separately, right after adding the NaOH solution to the reacting mixture (see above paragraph). The molecular structure of the dyes can be seen in Fig. 1. The molecules size was estimated using the program Gauss-View2.0. The drying temperature of the gels obtained was chosen to be lower than the decomposition temperature of the dyes in order to corroborate that the dyes were effectively trapped in the aluminosilicate matrix. In this way, the drying temperature was 523 K for the solid containing AL and 393 for the one containing CA, knowing that the corresponding decomposition temperatures for the dyes are 563 K and 411 K, respectively. In addition to these samples we also prepared a set of impregnated dry ground samples. In this latter case we impregnated separately CA or AL to the pure aluminosilicates in the same molar ratios, dry grounding the mixture in an agate mortar.

These samples were useful to establish differences (by using diffuse reflectance spectroscopy) between just smearing the dyes to the surface or promoting an effective encapsulation by using the in situ procedure.

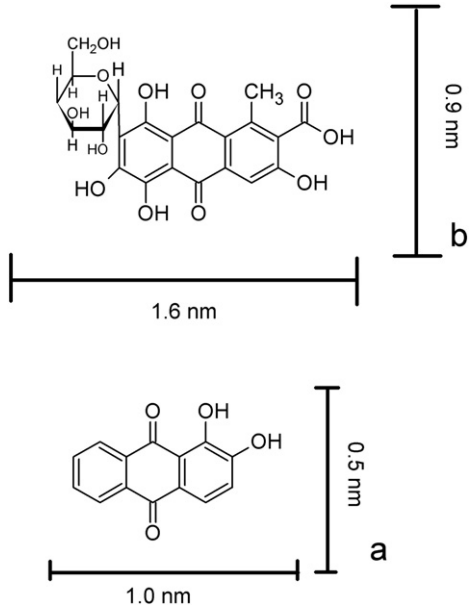

Fig. 1. Molecular structure and size of the dyes: a) 1,2-dihydroxyanthraquinone (alizarine) and, b) 7-α-D-glucopyranosyl-9,10-dihydro-3,5,6,8-tetrahydroxy-7-methyl-9,10-dioxanthracenecarboxylic acid (carminic acid).

2.4. Characterization

The X-ray Diffraction patterns were obtained using a Siemens D500 diffractometer with CuKα radiation (λ = 1.5406 Å) and a diffracted beam monochromator. Compounds were identified in the conventional way using the JCPD files. The diffractograms were not smoothed, then it may happen that the signal to background ratio in the figures shown in this manuscript is not as good as it could be, but in this way no information is lost. This effect is more pronounced in the thermodiffraction experiments as the diffractograms were recorded in situ; i.e., gradually heating the sample at the chosen temperature. Indeed, atom positions are less defined due to the thermal agitation.

Radial Distribution Functions (RDF) were obtained from X-ray Diffraction patterns measured with a molybdenum anode tube; only in this way it was possible to reach the required high values of the angular parameter. The intensity was measured by step scanning at an angular interval of 2θ = 0.1° up to 2θ = 120°. These data were the input for the Radiale program [24].

Small Angle X-ray Scattering (SAXS) experiments were performed using a Kratky camera coupled to a copper anode X-ray tube which K-α radiation was selected with a nickel filter. The collimated X-ray beam was linear and corresponded to an 'infinitely high' beam. The SAXS data, collected with a proportional linear counter were processed with the ITP program [25–28] where $I(h)$ is the intensity and the angular parameter, h in $Å^{-1}$ is defined as $h=(4\pi\sin\theta)/\lambda$, where θ and λ are the scattering angle and the X-ray wavelength, respectively. Measurement time was 9 min in order to obtain acceptable statistic results.

The shape of the scattering objects was estimated from the Kratky plot; i.e. $h2I(h)$vs h. From this plot it is possible to assess if the shape is fibrillar or globular. If the Kratky curve presents a broad peak, the scattering objects most probably present a globular conformation, whereas if the curve approximates a plateau the particles most probably are fibril-like objects [29,30]. The Log $I(h)$ vs Log h plot provides the fractal dimension value [31–33], still it has to be made in the linear zone of the plot $0.05<\text{Log } h<0.15$ which corresponds to the nanometrical scale.

The diffuse reflectance measurements were done using the labsphere RSA-PE-20 accessory.

In this latter case the samples were diluted with $BaSO_4$ before the study. The spectra were recorded in the 400–800 nm regions. The spectra

were interpreted using pure dyes and non impregnated aluminosilicate as reference materials.

A Bruker ASX-300 spectrometer was employed at a resonance frequency of 78.15 MHz to obtain the ^{27}Al MAS NMR signals using a solution of $Al(NO_3)_3$ as an external reference. Bands were attributed from the already reported results in the bibliography.

The sample SX was analyzed in a quantachrome autosorb automated gas sorption system to obtain the nitrogen adsorption isotherm at 77.4 K. The sample was outgassed at 573 K for 1 h prior to analysis. The specific surface area was estimated with the Brunauer–Emmet–Teller (BET) model and the pore size distribution was evaluated with the BJH model. The attenuated total reflectance Fourier infrared (ATR/FTIR) spectra were obtained in a GX Perkin Elmer instrument at 2.0 cm^{-1} resolution of 4000–400 cm^{-1}. Bands were attributed by comparison with the spectra already reported in bibliography.

3. Results

3.1. Preliminary results

According to the diffuse reflectance analyses the aluminosilicates SA and SY did not adsorb significant amounts of any of the organic dyes via in situ; see Fig. 2a and c, where the corresponding bands in the visible region assigned to the encapsulation of AL were very weak. Taking into account these results, we decided to study only samples prepared using the aluminosilicate SX as an adsorbent. The relevant results appear in the following sections.

3.2. X-ray Diffraction (XRD)

The diffractogram of sample SX indicated that an amorphous powder was obtained at 298 K; see Fig. 3a. A thermal study was performed in situ on the same sample, in order to demonstrate the thermal stability of the aluminosilicate SX. This was done gradually heating a sample up to 1273 K. Corresponding results are shown for the sample treated at 773 K (Fig. 3b) and 1273 K (Fig. 3c), respectively. The amorphous structure was maintained during the whole continuous treatment as shown by the absence of sharp diffraction peaks in the sample. The peak at 2θ ca. 40° and marked with an asterisk is due to the sample holder. At 1273 K however, the sample begins to crystallize, as shown by the small peak at 2θ ca. 11° assigned to nepheline, which is a zeolite with a two dimensional pore system. Note that nepheline is stable below 1521 K and it may crystallize at 773–973 K, depending on the environment.

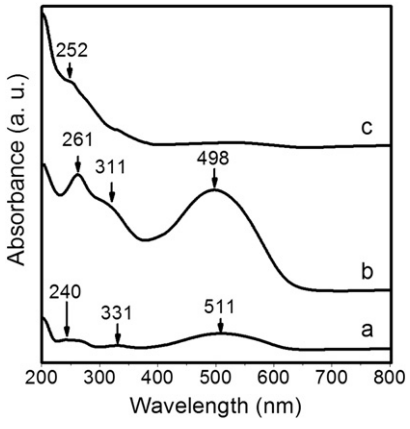

Fig. 2. Diffuse reflectance spectra of aluminosilicates impregnated in situ with AL and dried 24 h in air at 523 K: a) sample SA, b) sample SX and, c) sample SY.

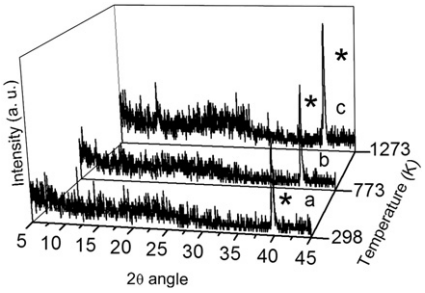

Fig. 3. X-ray diffractograms of aluminosilicate SX at: a) 298 K, b) 773 K and, c) 1273 K.

3.3. FTIR

The FTIR spectra of sample SX are presented in Fig. 4. In Fig. 4a, the sample at 298 K is shown. A wide band appears at 3440 cm^{-1}, assigned to M–OH stretching (M: Si, Al, Mg) [34]. Weak bands appear at 2924 and 2850 cm^{-1}, corresponding to C–H stretching bands [35], from residual reactants such as alkoxides and 2-BuOH. A sharp band appears at 1636 cm^{-1} corresponding to the deformation band from H_2O [36]. A weak but well defined band at 1404 cm^{-1} corresponds to C–O stretching [35]. A strong wide band at 1032 cm^{-1} can be assigned to asymmetric M–O–M stretching. A well defined wide band at 690 cm^{-1} corresponds to M–O stretching. Finally, a band at 450 cm^{-1} appears, corresponding to a MO–M rocking vibration [35].

Fig. 4b shows the FTIR spectrum of the sample SX calcined at 773 K. There occurs a significant reduction in the amount and intensity of the bands. Specifically, the bands at 3400 and 1643 cm^{-1} are weaker compared to those in Fig. 4a, indicating surface dehydroxilation [1]. A sharp band appears at 1004 cm^{-1} corresponding to M–O–M stretching. Two other bands at 692 and 431 cm^{-1} also appear, corresponding to M–O vibrations. The spectrum in Fig. 4c corresponds to sample calcined at 1273 K, showing a totally dehydroxylated surface, where the bands at 3400 and 1643 cm^{-1} have disappeared. According to the literature, bands

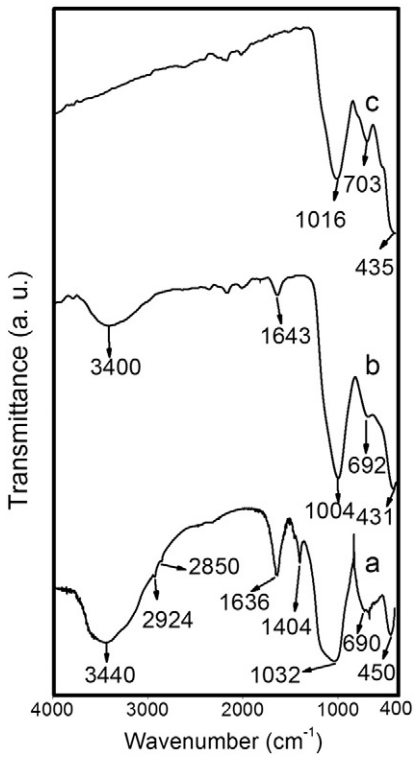

Fig. 4. FTIR spectra of aluminosilicate SX at: a) 298 K, b) 773 K and, c) 1273 K.

at 1090, 700, 513 and 472 are typical of nepheline [37]. In this way, we can attribute the bands at 1016, 703 and 435 cm^{-1} in Fig. 4c to nepheline.

3.4. Radial distribution functions (RDF)

The radial distribution function of sample SX dried at 523 K is presented in Fig. 5a. This function has been discussed in a previous work where the sample was impregnated with cationic organic dyes [38]. The material is constituted by chains of TO_4 where T is a Si or Al atom in the tetrahedral building unit of the aluminosilicate, the peak located at a radial distance of 0.17 nm is due to the T–O distance, the one at 0.23 to O–O and the one at 0.34 to T–T distances. The peaks at 0.44 and 0.50 nm may be attributed to the interatomic distances, corresponding to the second neighbors, O–O and T–T. These peaks differ, within experimental error (+0.05 nm), with those reported by other authors for vitreous SiO_2 [39]:

Si–O = 0.16, O–O = 0.27, Si–Si = 0.32, Si–O = 0.40, for the tetrahedral distances and O–O = 0.45, Si–Si = 0.52 nm for the second neighbors. The interatomic distances corresponding to Mg–O can be estimated from the ionic radii, and they turn out to be 0.19 nm (coordination of Mg = 4) or 0.21 nm if a coordination of 6 is assumed. They cannot be resolved from the very close distances of 0.16 nm corresponding to Si–O or 0.17 corresponding to Al–O.

Hence, peaks found at 0.17 and 0.23 corresponding to T–O and T–T distances where T may be either Si or Al overlap the Mg–O distance. Mg, then, is assumed to be incorporated to the aluminosilicate matrix. The corresponding distribution function obtained for sample SX impregnated in situ with CA and dried at 393 K appears in Fig. 5b. Interestingly, it reproduces the radial distribution function already reported for SX sample up to 1.0 nm, although the powder impregnated with CA is light pink in color, compared to SX, which is a white powder.

Apparently a very small amount of CA is sorbed on the surface or trapped inside the cavities of the porous solid, whose structure is maintained. Indeed, none of the peaks of CA (a red color powder), Fig. 5d, appear in the impregnated sample, Fig. 5b. A different result was obtained for the reddish color sample, impregnated in situ with AL and dried at 523 K, see Fig. 5c. In this case, the initial radial distance of 0.17 nm corresponding to T–O is shifted to 0.19 nm; this value corresponds to the peak at 0.19 found in the AL radial distribution function, Fig. 5e, the first peak, then, includes T–O, Mg–O and AL first neighbor distances. The distance appearing at 0.23 nm in the SX sample and corresponding to O–O bonds, is located now at 0.24 nm, showing some relaxation of the O8 O skeleton. The peak at 0.32 can be attributed to AL molecule which shows a clear interatomic distance at 0.33 nm in Fig. 5e. The peak at 0.36 nm must be the shifted peak found at 0.34 nm in the original material and attributed to T–T distances which define the average angle between adjacent tetrahedra, estimated to be ca. 180° [39]. This shifting shows that the angle between TO_4 tetrahedra is different. Two new peaks appear at 0.43 and 0.49 nm. Again, the peak at 0.43 nm in Fig. 5c can be assigned to the modification of the original aluminosilicate structure by the complete encapsulation of AL (an orange-yellow powder) in the lattice of SX. The peak at 0.49 nm in Fig. 5c corresponds to AL, as it also appears in Fig. 5e, therefore AL maintains its structure even being encapsulated into the SX network.

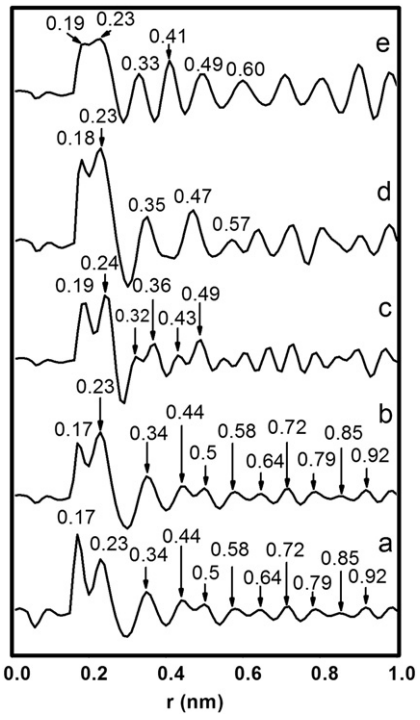

Fig. 5. Radial distribution function results of samples dried in air 24 h: a) amorphous aluminosilicate (sample SX) dried at 523 K, b) sample impregnated in situ with carminic acid (sample SXCA) dried at 393 K, c) sample impregnated in situ with alizarine (sample SXAL) dried at 523 K, d) carminic acid (CA), and, e) alizarine (AL).

3.5. Diffuse reflectance

The results can be seen in Fig. 6. The sample SX appears in Fig. 6a. No bands in the visible region were obtained as the powder is white in color. Comparing the sample impregnated with AL via in situ (Fig. 6b) to the one impregnated dry ground using mortar and pestle, (Fig. 6c) an important difference was found: The band centered at 498 nm in Fig. 6b appears more intense in Fig. 6c., centered at 486 nm. On the other hand, a very weak band appeared in the sample impregnated with CA via in situ around 573 nm; Fig. 6d, whereas it is slightly more intense for the sample impregnated dry ground at 567 nm; see Fig. 6e.

3.6. Small Angle X-ray Scattering (SAXS)

The results obtained for some samples appear in Fig. 7. The sample SX, plot Log $I(h)$ vs Log h, appears in Fig. 7a, having a fractal dimension of 2.90. Fig. 7b and c correspond to SX impregnated in situ with AL (fractal dimension 1.90) and CA, (fractal dimension 2.00) respectively. The corresponding Kratky plots (not shown here), exhibited the typical shape for a lamellar morphology in all cases. The scattering objects in these cases are pores, as they are altered by the dyes' adsorption. The pore size distribution of sample SX presented in Fig. 8a is broad and the maxima are located at r = 9.9 and 11.1 nm. The pore size distribution remaining after the adsorption of AL appears in Fig. 8b, showing maxima at r = 1.00, 3.1, and 5.9 nm. We assume that

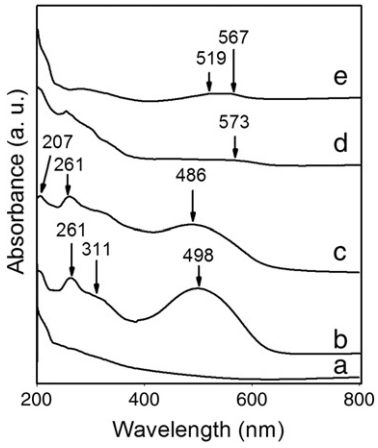

Fig. 6. Diffuse reflectance spectra of samples dried in air 24 h: a) SX, b) impregnated in situ with AL (523 K), c) impregnated dry ground with AL (523 K), d) impregnated in situ with CA (393 K) and, e) impregnated dry ground with CA (393 K).

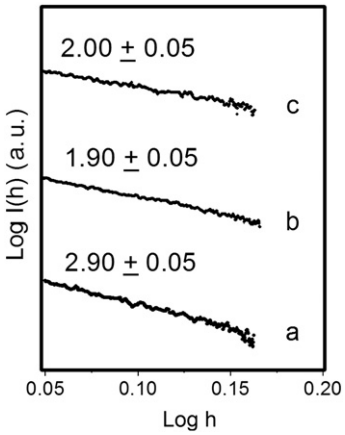

Fig. 7. Fractal dimension plots from SAXS of samples dried in air 24 h: a) SX (523 K), b) SX impregnated in situ with AL (523 K) and, c) SX impregnated in situ with CA (393 K). The error bars indicate the standard deviation from a least-square fit to a log/log straight line.

the AL molecules fill mainly large, but also some small matrix pores, considering that the AL molecule size is between 0.5 and 1.0 nm; see Fig. 1a. Regarding sample SX impregnated with CA, the resulting pore size distribution appears in Fig. 8c. The maxima are at 0.97, 3.5 and 6.6 nm. In this case, due to the larger dye molecule size, which is between 0.9 and 1.6 nm (see Fig. 1b), the CA molecules occupy only the largest cavities, as expected.

3.7. ^{27}Al MAS NMR

In all the spectra (not shown here), two signals were obtained: an intense one at 57 ppm attributed to tetrahedral Al and a weak signal at 5 ppm, attributed to octahedral Al species. The signal at 57 ppm is related to the interaction of Al in the vicinity of Si in the matrix and it is associated to the formation of Al – O – Si bonds in tetrahedral structures. The signal at 5 ppm is related to the formation of aluminum hydroxide, $Al(OH)_3$, microdomains disperse in the oxide matrix.

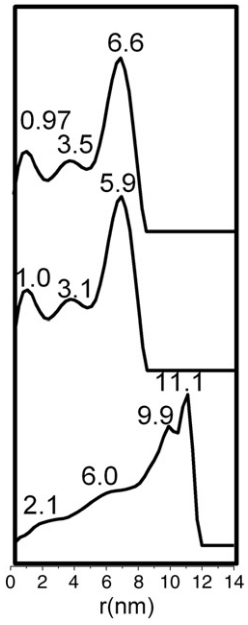

Fig. 8. Pore size distribution calculated from SAXS measurements of samples dried in air 24 h: a) SX (523 K), b) impregnated in situ with AL (523 K) and, c) impregnated in situ with CA (393 K).

3.8. Nitrogen physisorption

The nitrogen adsorption–desorption isotherm of sample SX has been reported previously elsewhere [38]. The obtained shape corresponds to a type IV isotherm according to the IUPAC classification. The hysteresis loop in the isotherm (not shown here) can be attributed to the presence of open pores where no condensation is evident; therefore, inkbottle shaped pores have to be discarded [38]. According to the results obtained by this technique, the pore diameter varies between 5 and 8 nm (results not shown here). The corresponding surface area was 170.1 ± 1.4 m^2/g.

4. Discussion

We consider the following three factors as the most important in our research: 1) the overall chemical composition (including the compensation cations Na^+ or Mg^{+2}), 2) the Si/Al molar ratio and, 3) the r value, where r: mol H_2O/mol T (T: Al^{+3}, Si^{+4}) and, 4) the fractal dimension and porosity. These are the influential variables in the efficiency of aluminosilicates SA, SX or SY as organic dye adsorbents, which differ in the cavities size and electrostatic attraction.

Our results show that the sample SX is constituted by an amorphous compound where Mg^{+2} cations are included in the network (XRD and RDF results); no Mg crystalline compounds were observed. Again, when interacting with AL or CA no new crystalline or amorphous compounds are formed. It seems that the dye structure is maintained in both cases. Mg^{+2} cations play an important role in the stabilization of dyes in the matrix cavities (samples SX and SY), as they compensate the charges originated by the replacement of silicon by aluminum in the aluminosilicate structure. Divalent cations in a FAU zeolite type structure propitiate centers positively charged which may interact strongly with the anionic dyes.

Instead, monovalent cations propitiate a homogeneous charge distribution and they are not prone to interact with the dye. The intense band of sample X impregnated via in situ with AL at 498 nm compared to the corresponding one at 486 nm obtained in the sample impregnated dry ground (see Fig. 6b and c) can be explained because in the first one the AL molecules are trapped inside the matrix cavities either as single molecules or olygomers, whereas for the latter one, most molecules are mainly deposited as microcrystals on the surface. Such a significant difference between the samples impregnated with CA (see Fig. 6d and e) was not found, as in both cases a very weak band appeared at 573 and 567 nm, respectively. In these samples the CA molecules were mainly sorbed as aggregates onto the surface. From these results, we consider that AL has been effectively encapsulated in the matrix, whereas CA was mainly impregnated on to the surface.

The pore size distributions obtained by SAXS confirmed these results, showing smaller pores in the sample impregnated with AL compared to sample impregnated with CA; see Fig. 8b and c, respectively. Another remarkable result was the stability of the trapped dyes. In spite of repeated Soxhlet extractions during 24 h of the impregnated samples using 2-BuOH as solvent, none of the molecules either AL or CA could be extracted. The resulting solutions did not contain any detectable amount of the dyes. This was proven using UV–Vis spectroscopy. In this way, the organic molecules were bonded to the aluminosilicate cations. These results are in agreement with those reported by Ibarra et al. and Marqués et al. [22,23].

In sample SA the molar ratio Si/Al = 1.0, whereas in sample SX and SY the corresponding values are 2.25 and 14.0, respectively. Hence, it is expected that the hydroxylation degree of those samples should be higher in SY and lower in SA. Although sample SX maintained an amorphous structure from room temperature and up to almost 1273 K, the surface showed several changes, as it was demonstrated by FTIR spectroscopy. The evolution consisted on the surface dehydroxylation, the elimination or organic residue and the crystallization of nepheline. The dehydroxilation may also be attributed to the temperature effect on

the microdomains of aluminum hydroxide, $Al(OH)_3$, detected by NMR in sample SX.

The r value also proved to be critical in the hydrolysis–condensation process. The r values employed to synthesize our aluminosilicates were: 30.7 for SA, 3.7 for SX and 20.7 for SY. The initial hydrolysis step was better controlled in the synthesis of sample SX, where r = 3.7, whereas in the other cases the growth of oligomers was randomly due to the great amount of H_2O used. Thus, sample SX is the only appropriate adsorbent to host AL or CA. The fractal dimension results of SX sample impregnated in situ with AL or CA can be explained referring to a growth of tetrahedral oligomeric T–O–T (T: Al, Si) species, where the organic dye molecules played an important role related to a steric hindrance. In this way, most of the Al species were tetrahedral, instead of octahedral [22]. Indeed, a strong resonance at 57 ppm was observed in the ^{27}Al MAS NMR spectra (spectra not shown here) [22].

A weak resonance also appeared at 5 ppm, indicating the presence of a small amount of octahedral Al species. In this way, the samples, impregnated with AL (Fig. 7b) or CA (Fig. 7c), have similar fractal dimension values; 1.90 and 2.00, respectively. On the other hand, in pure sample SX, the growth mechanism seemed to be different, resulting in a fractal dimension value of 2.90, where the material is denser as no dye molecules are present during the polymerization step. Such conclusion has been confirmed by ourselves comparing the spectra of an AL solution (1% mol in 2-BuOH; spectrum not shown here) and SX impregnated in situ with AL. In the first case a band at 435 nm appears, whereas for the latter one the band appears at 498 nm (see Fig. 6b). The $\Delta\lambda = 63$ nm batochromic shifting can be attributed to the confining of AL aggregates inside the aluminosilicate matrix in the in situ sample and is due to the AL π-π^* electronic transition [40].

5. Conclusions

Amorphous aluminosilicates SA, SX, SY were synthesized via the sol–gel process. Only sample SX, with the nominal composition $Na_{12}Mg_{23}(Al_{59}Si_{133}O_{384})\cdot 26H_2O$ proved to be appropriate to be used as a sorbent material. The aluminosilicate was amorphous in the range 298 K up to ca. 1273 K. At this latter temperature however, the sample begins to crystallize as nepheline, which is a zeolite with a two dimensional pore system. AL was successfully encapsulated inside the matrix pores via the so-called in situ procedure. CA was found to be deposited on the matrix surface, due to its larger size. The dye sorption was proved by several experimental techniques.

Acknowledgments

We would like to thank CBI research lab of Universidad Autónoma Metropolitana-Iztapalapa for sharing the equipment. Orlando Martínez-Zapata also thanks the CONACyT for the financial support, scholarship no. 198165, provided to achieve his PhD.

References

[1] C.J. Brinker, G.W. Scherer, Sol–Gel Science, The Physics and Chemistry of the Sol–Gel Process, Academic Press, San Diego, CA USA, 1990.
[2] D. Avnir, Acc. Chem. Res. 28 (1995) 328–334.
[3] J. Livage, CR Acad. Sc. Paris 322 (1996) 417.
[4] D. Levy, Chem. Mater. 9 (12) (1997) 2666–2670.
[5] C. Sanchez, B. Lebeau, F. Ribot, M. In, J. Sol-Gel Sci. Tech. 19 (2000) 31–38.
[6] Y. Yin, C. Wang, C. Wang, J. Sol-Gel Sci Tech. 48 (2008) 308–314.
[7] S. Kowalak, A. Jankowska, Microporous Mesoporous Mater. 61 (2003) 213–222.
[8] G. Atun, G. Hisarli, Chem. Eng. J. 95 (2003) 241–249.
[9] A.B. Mukhopadhyay, C. Oligschleger, M. Dolg, J. Non-Cryst. Solids 351 (2005) 1151–1157.
[10] Y. Li, Q. Yang, J. Yang, C. Li, J. Porous Mater. 13 (2006) 187–193.
[11] D.W. Breck, Zeolite Molecular Sieves, John Wiley & Sons, New York, 1974.
[12] H. Laguna, S. Loera, I.A. Ibarra, E. Lima, M.A. Vera, V. Lara, Microporous Mesoporous Mater. 98 (2007) 234.
[13] Z. Ni, S. Xia, L. Wang, F. Xing, G. Pan, J. Colloid Interface Sci. 316 (2007) 284.
[14] D.N. Bakoyannakis, G.A. Stdidis, D. Zamboulis, D.A. Jannakoudakisb, J. Chem. Technol. Biotechnol. 58 (2007) 247.
[15] S. Kowalak, A. Jankowska, S. Zeidler, S. Wieckowski, J. Solid State Chem. 180 (2007) 1120–1124.
[16] R.J.H. Clark, T.J. Dines, M. Kurmoo, Inorg. Chem. 22 (1983) 2766–2772.
[17] S. Kowalak, A. Jankowska, S. Zeidler, Microporous Mesoporous Mater. 93 (2006) 111–118.
[18] E. Lima, M.J. Martínez-Ortíz, E. Fregoso, J. Méndez-Vivar, Stud. Surf. Sci. Catal. 170 (2007) 2110–2115.
[19] S. Murcia-Mascaro, C. Domingo, S. Sanchez-Cortes, M.V. Canamares, J.V. Garcia-Ramos, J. Raman Spectrosc. 36 (2005) 420.
[20] S.N. Meloan, L.S. Valentine, H. Puchtler, Histochem. Cell Biol. 27 (1978) 87.
[21] P. Schmitt, H. Giinther, G. Hagele, R. Sake, Org. Magn. Reson. 22 (2005) 14.
[22] I.A. Ibarra, S. Loera, H. Laguna, E. Lima, V. Lara, Chem. Mater. 17 (2005) 5763.
[23] B. Marqués, S. Leiva, A. Cantín, J.L. Jordá, M.J. Sabater, A. Corma, S. Valencia, F. Rey, Stud. Surf. Sci. Catal. 174 (2008) 249.
[24] M. Magini, A. Cabrini, J. Appl. Crystallogr. 5 (1972) 14.
[25] O. Glatter, J. Appl. Crystallogr. 14 (1981) 101.
[26] O. Glatter, J. Appl. Crystallogr. 17 (1984) 435–441.
[27] O. Glatter, Prog. Colloid Polym. Sci. 84 (1991) 46–54.
[28] O. Glatter, B. Hainisch, J. Appl. Crystallogr. 17 (1984) 435–441.
[29] M. Kataoka, Y. Hagihara, K. Mihara, Y. Goto, J. Mol. Biol. 229 (1993) 591–596.
[30] T. Tono, M. Kataoka, Y. Kamatari, K. Kanaori, A. Nosaka, K. Akasaka, J. Mol. Biol. 251 (1995) 95–103.
[31] A. Harrison, Fractals in Chemistry, Oxford University Press, UK, 1995.
[32] J.E. Martin, A.J. Hurd, J. Appl. Crystallogr. 20 (1987) 61–78.
[33] A. Barrera, M. Viniegra, V.H. Lara, P. Bosch-Giral, Catal. Commun. 5 (2004) 569–574.
[34] C. Lin, J.D. Basi, in: A.K. Cheetham, C.J. Brinker, M.L. Mc Cartney, C. Sanchez (Eds.), Mat. Res. Soc. Symp. Proc., 73, 1986, p. 585, Pittsburgh PA.
[35] K. Nakamoto, Infrared and Raman Spectra of Inorganic and Coordination Compounds, Part A, Fifth Edition John Wiley & Sons Inc., NY, 1997.
[36] P. Pramanik, S.K. Saha, J. Elastomers & Plastics 23 (1991) 345–361.
[37] D.V. Makarov, A.T. Belyaevskii, D.P. Nesterov, M.F. Yusupova, Russ. J. Appl. Chem. 80 (2007) 175.
[38] O. Martínez-Zapata, J. Méndez-Vivar, P. Bosch, V.H. Lara, J. Non-Cryst. Solids 355 (2009) 2496–2502.
[39] H. Klug, L. Alexander, X-Ray Diffraction Procedures, John Wiley, New York, 1954.
[40] M. Rouila, A.A. Vassiliadis, J. Colloid Interface Sci. 291 (2005) 37–44.